Pressure Dependence of the Intramolecular Electron Transfer Reaction in Myoglobin Reinvestigated

Yoshiaki Furukawa, Koichiro Ishimori, and Isao Morishima*

Department of Molecular Engineering, Graduate School of Engineering, Kyoto University, Kyoto 606-8501, Japan

Received: June 4, 1999; In Final Form: December 6, 1999

The activation volumes ($\Delta V^{\neq}$) for intramolecular electron transfer (ET) reactions in Ru-modified Zn-porphyrin (ZnP) substituted myoglobins (Ru−ZnMb) have been determined to investigate the pressure effects on the redox potentials and donor−acceptor distance (D−A distance) for the ET reaction. Three Ru−ZnMbs, in which D−A distances for the ET reactions are 12.7 Å (His48Mb), 15.5 Å (His83Mb), and 19.3 Å (His81Mb), were constructed. The activation volumes for the forward ET reactions ($\Delta V^{\neq}_{f}$) were −1.6 (His83Mb), +3.7 (His81Mb), and +6.5 cm^3 mol^{-1} (His48Mb). We also measured the pressure dependence of the back ET reactions (from Ru^{2+} complex to ZnP^+), showing that the back ET reactions exhibited negative activation volumes ($\Delta V^{\neq}_{b}$) for all of the Ru−ZnMbs: −11, −5.3, and −6.2 cm^3 mol^{-1} for His83Mb, His81Mb, and His48Mb, respectively. On the basis of these activation volumes, the pressure dependence of the redox potentials, $(\partial\Delta G°/\partial P)_T$, was estimated as about 2.94×10^{-4} eV MPa^{-1}, regardless of the position of the Ru complex. Since $(\partial\Delta G°/\partial P)_T$ in the present study is close to that of $Ru(NH_3)_6^{2+/3+}$ (2.97×10^{-4} eV MPa^{-1}), the pressure-induced redox changes of the Ru complex were primarily responsible for that of the ET reaction and the contribution of ZnP to the pressure dependence of the redox potential on the ET reactions would be small. In sharp contrast to $(\partial\Delta G°/\partial P)_T$, the pressure dependence of the D−A distance, $(\partial d/\partial P)_T$, highly depends on the ET pathway and microenvironments of the redox centers. The linear compressibility, $(-1/d_0)(\partial d/\partial P)_T$, was $(2.2 \pm 0.1) \times 10^{-10}$, $(5.1 \pm 0.5) \times 10^{-11}$, and $(-2.6 \pm 3.2) \times 10^{-11}$ m^2 N^{-1} for His83Mb, His81Mb, and His48Mb, respectively. The different linear compressibility for the three ET reaction systems suggests that the structural fluctuation in proteins is not unique in protein structure and site specific local fluctuations would be one of the factors regulating the protein ET reactions.

Introduction

Electron transfer (ET) reactions play essential roles in several important biological processes, including photosynthesis and respiration.[1] In recent years, interest in understanding of ET reactions for metal enzymes has significantly increased, since new theories and techniques which provide us with various information of the factors regulating the ET reaction in proteins can be available.[2,3] It is in this respect that the effects of protein dynamics on ET processes in protein have received considerable attention.[4−8] As previously reported in many protein systems,[2,3] the static structure of a protein, deduced from the crystallographic analysis, would not be enough to characterize the ET reactions. In addition to the static structure of proteins, the contribution of dynamic motions of proteins would be essential for the ET reactions in proteins, because the structural fluctuation by the thermal motions of proteins affects the relative position of the redox centers and amino acid residues on the ET pathway.[9,10] Aquino et al.[7] theoretically examined the effects of dynamic fluctuations on the ET reaction between cytochrome c_2 and the photosynthetic reaction center and suggested that the specific protein fluctuation could enhance the ET rates. Daizadeh et al.[8] also carried out computer simulations of effects of protein dynamics on the ET reaction and proposed that vibrational motion of the ET pathway regulates the protein ET reaction. Although these theoretical studies predict that the thermodynamical fluctuation plays a substantial role in the ET reaction, only few experimental studies paying attention to the effects of thermodynamical fluctuation on the ET process in protein have been reported.

To examine the significance of fluctuation in ET reactions, we have paid our attention to the pressure effects on the ET rates.[11] As previously shown,[12−14] pressurization increases the material density and number of collisions between molecules, leading to suppression of the thermodynamical fluctuation. Our group and other groups have previously investigated the pressure dependence on the intramolecular ET rates for myoglobin (Mb)[11] and cytochrome c[15−17] and b_5 derivatives.[18] In cytochromes, the ET rates were accelerated by pressurization or almost independent of pressure, which has been explained by distance contractions between donor and acceptor sites under high pressure.[15,18] In the case of Ru-modified Zn-substituted Mb (Ru−ZnMb) derivatives, our preliminary study[11] showed the significant deceleration of the ET rates by pressurization, which could not be explained by the simple distance contractions. We reported that the positive activation volumes of the ET reactions in Ru−ZnMb derivatives increased with increasing donor−acceptor (D−A) distance, which allowed us to introduce the effects of the structural fluctuation into the Marcus equation and propose the protein fluctuation controlled ET mechanism.

Although the ET rate constants in our previous study[11] were highly reproducible under the condition we employed, we found

* To whom correspondence should be addressed. Phone: +81-75-753-5921. Fax: +81-75-751-7611. E-mail: morisima@mds.moleng.kyoto-u.ac.jp.

10.1021/jp991813g CCC: $19.00
Published on Web 02/04/2000

SCHEME 1

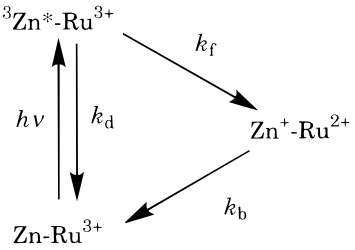

that the extensive replacement of dissolved oxygen with argon by using a vacuum argon line, instead of the glovebox as conducted in our previous experiment, reduced the ET rates. In other words, dissolved oxygen molecules in the sample enhanced the decay of the triplet excited state of ZnMb (^{3}Zn*Mb).[19−21] The contamination of O_2 in the previous sample preparation, therefore, gave the larger "apparent" ET rate than the "real" ET rate from ^{3}Zn*Mb to the Ru complexes. In this study, we present refined experimental data on the ET rate constants and the activation volumes under anaerobic condition to reexamine the protein fluctuation controlled ET mechanism we previously proposed.

With the refinement of the data on the ET rate constants from ^{3}Zn*Mb to the Ru^{3+} complex, we also examined the "back ET process" from the Ru^{2+} complex to the cation radical of Zn-mesoporphyrin (Scheme 1) to discuss the ET reactions in Ru−ZnMbs in more detail. As Gray and co-workers have reported,[22,23] the "back ET process" serves as another model for the ET reaction in proteins. The back ET process has a different driving force for the reaction from that of the forward ET process,[24] which may offer an attractive alternative for evaluating the effects of the structural fluctuation on the ET process in proteins. In this paper, by utilizing high-pressure laser flash photolysis, we have elucidated the pressure dependence of the back ET process in three Ru−ZnMbs having different D−A distances. Particularly, we focused on the pressure dependence of the redox potential and D−A distance in the Mb systems, both of which have been considered to be crucial factors to control the ET process[1] and were not examined in the previous paper.[11] Together with the results from the forward ET process, we further discussed the effects of structural fluctuation on the ET process in proteins in more detail.

Materials and Methods

Chemicals. All DNA-modifying enzymes were purchased from Wako and nacalai tesque. All chromatographic products such as DEAE-Sepharose, Sephadex G-25, and HiTrap SP cation-exchange columns were purchased from Pharmacia. Chloropentaammineruthenium(III) dichloride, $[Ru(NH_3)_5Cl]Cl_2$, from Sigma was used for the experiments, and other chemical reagents were the analytical grade. Deionized water purified by the Barnstead NANOpure II water purification system was used in the preparation of all aqueous solutions.

Preparation of Aquopentaammineruthenium(II). Aquopentaammineruthenium(II), $Ru(NH_3)_5(H_2O)^{2+}$, was prepared by reduction of $[Ru(NH_3)_5Cl]Cl_2$ as previously reported.[25] $[Ru(NH_3)_5Cl]Cl_2$ was reduced by zinc amalgam, and the product was precipitated as the hexafluorophosphate salt and stored under vacuum. The product was checked by EI-mass spectrometry (results not shown) and confirmed as $Ru(NH_3)_5(H_2O)^{2+}$.

Preparation of Zinc Mesoporphyrin IX Diacid. Mesoporphyrin IX dimethyl ester (ca. 50 mg) was first saponified to the diacid by refluxing in methanol containing KOH and water.

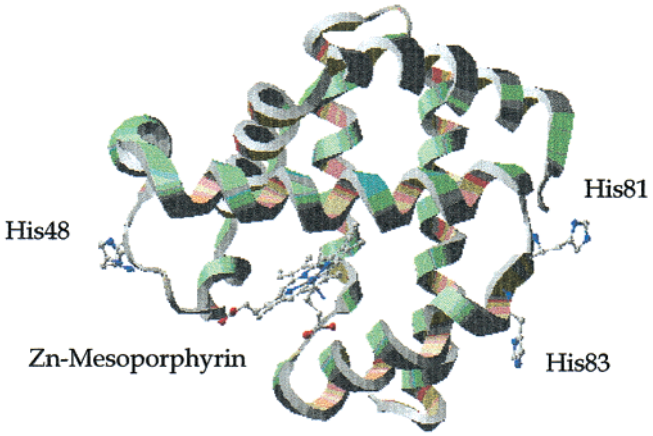

Figure 1. Positions of the Ru-modified histidines and Zn-substituted porphyrin in human Mb.

A zinc(II) complex of mesoporphyrin IX diacid (ZnP) was prepared by the method of Adler et al.[26] The purity of the product was checked by thin-layer chromatography and ^{1}H NMR spectra (results not shown). No additional bands and signals were observed. ZnP was stored in a foil-wrapped vial at −80 °C.

Preparation of Ruthenated Myoglobins. Human Mb used in this study has a mutation at Cys 110 (Cys → Ala) to avoid dimer formation during the purification.[27] The procedures for the site-directed mutagenesis are described elsewhere in a previous paper.[22] Human Mb has two accessible histidines on its surface (His48 and His81) against the Ru modification.[22] To construct the singly Ru modified Mbs as illustrated in Figure 1, the H48N, H81N, and H48N/H81N/E83H human Mb genes were constructed, in which the accessible histidine on the protein surface is limited to His 81, His 48, and His 83, respectively. The D−A distance (distance between Ru complex and ZnMP), which is calculated from the edge to edge, is 15.5, 19.3, and 12.7 Å for H48N/H81N/E83H Mb (His83Mb), H48N Mb (His81Mb), and H81N Mb (His48Mb), respectively. All DNA sequencing was done by the DyeDeoxy Terminator method using ABI 373S DNA sequencer (Perkin-Elmer). Protein preparation and purification were performed by the method described previously.[28,29]

A solution containing 70 mg (3.3 mL, 1.3 mM) of Mb mutants (aquomet form) in 10 mM sodium phosphate buffer, pH 7.0, was degassed and purged with argon. A 25-fold excess of solid $Ru(NH_3)_5(H_2O)^{2+}$ was added to the Mb solution under an argon atmosphere. The ferric Mb was immediately reduced to the ferrous state, and the color of the solution changed from brown to deep red. After the incubation for 3 h at room temperature, the mixture was oxidized by addition of an excess amount of ferricyanide and loaded onto a Sephadex G-25 column (2 cm × 10 cm) equilibrated with 50 mM sodium phosphate, pH 5.5, to remove the excess Ru complex and ferricyanide. The protein fractions were collected and concentrated by ultrafiltration to ca. 2 mL.

The ruthenated Mb samples were separated and purified from the reaction mixture by passing through a HiTrap SP (1 mL) cation-exchange column fitted to a Pharmacia FPLC system.[22] The samples were loaded in buffer A (50 mM sodium phosphate, pH 5.5) and eluted by a linear gradient of buffer B (50 mM sodium phosphate, pH 6.5, 1 M NaCl). Starting with 0% buffer B, the contents of the B buffer increased to 100% after 50 min with a flow rate 1.0 mL/min. Ru-unmodified Mb was not adsorbed on the column in 50 mM sodium phosphate, pH 5.5.

The fractions containing the purified Ru-modified Mb derivative were pooled and concentrated by Amicon ultrafiltration to ca. 2 mL.

Preparation of Zinc-Substituted Ruthenated Myoglobins. To prepare apoprotein, the heme was removed from Ru-modified Mb by the acid−butanone method.[30] After the pH of the ruthenated Mb solution (ca. 10 mL) was lowered to pH ca. 3.0, an equivolume of 2-butanone was added to the solution to extract the heme. The extraction was repeated twice, and the aqueous apoprotein solution was dialyzed against 5 L of 50 mM Tris−HCl, pH 8.0, for overnight.

The apoprotein solution was maintained at 4 °C in the reconstitution of ZnP. Approximately 2 mg of ZnP was dissolved into 1 mL of dimethylformamide, and the solution was added dropwise to the apoMb solution (ca. 20 mL) with gentle stirring. The reaction mixture was stirred for overnight in the dark at 4 °C.

The crude Ru-modified Zn-substituted Mb (Ru−ZnMb) was purified by a HiTrap SP cation-exchange column fitted to a Pharmacia FPLC system.[22] The samples were loaded on the column equilibrated with 50 mM sodium phosphate, pH 5.5, and eluted with a linear gradient of 50 mM sodium phosphate, pH 6.5, 1 M NaCl. The gradient was the same as the case of preparation of ruthenated Mb. Sample purity was confirmed by a A_{414}/A_{280} ratio of ca. 16, as previously reported.[31] All manipulations of Zn-substituted Mb (ZnMb) were performed in the dark. The modification of the Ru complexes to ZnMb can be confirmed by native-PAGE. The pI of Ru−ZnMb was higher (pI > 8.0) than that of Ru-unmodified ZnMb (pI 7.4).[24]

Measurements of the ET Rate Constants. UV/vis spectra were obtained by using a Shimadzu UV-2200 spectrophotometer at room temperature in 100 mM Tris−HCl, pH 7.4.

The decay of the triplet-excited state of ZnP in ZnMb (^{3}Zn*Mb) was monitored at 450 nm for the forward ET process, while, for the back ET process, that of the π-cation radical (Zn^+Mb) was followed by the absorbance at 380 nm, as previously reported.[22] The second harmonic (532 nm) of a Q-switched Nd:YAG laser provided photolysis pulses with a half-peak duration of 10 ns. The temperature was controlled by using a circulating water bath (±0.1 °C). In ambient pressure experiments, fully oxidized protein samples (2−5 μM protein concentration in 100 mM Tris−HCl, pH 7.4) were transferred into the vacuum cell having a 1 cm cuvette sidearm. The samples were degassed by using a vacuum-argon line to remove residual oxygen and purged with purified argon gas.[19,21] Kinetic data were averages of at least 50 laser shots. The absorption spectrum of ZnMb did not change after 3000 laser shots (figure not shown), which indicates that the Ru−ZnMbs are quite stable during the pulsed-laser experiments under anaerobic conditions.

The triplet decay rate, k_{obs}, for Ru−ZnMb after pulsed-laser excitation was, in principle, the sum of the intrinsic decay rate, k_d, and the ET rate constant, k_f, from ^{3}Zn*Mb to Ru^{3+} (forward ET), as expressed in[31]

$$k_{obs} = k_d + k_f \quad (1)$$

To obtain the ET rate constants (k_f), the intrinsic decay rate (k_d) of ^{3}Zn*Mb was estimated by using ZnMb without the Ru modification.

To obtain the back ET rate constants, k_b, the decay signal of Zn^+Mb was fitted by the following equation:[23,32]

$$\Delta A_{380} = A_1\{\exp(-k_{obs}t) - \exp(-k_b t)\} + A_2 \exp(-k_{obs}t) + A_3 \quad (2)$$

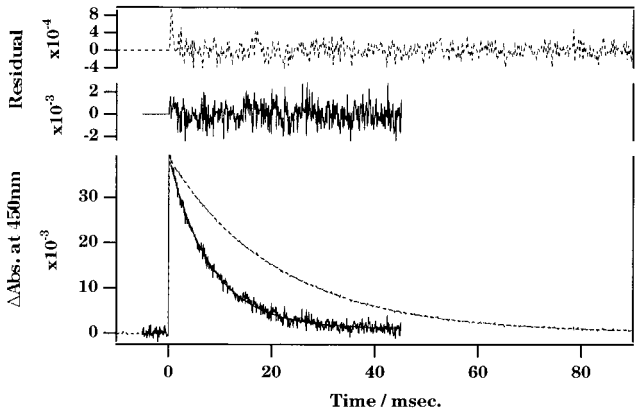

Figure 2. Transient absorbance changes at 450 nm obtained after laser excitation (532 nm; 10-ns pulse width) of ZnP in ZnMb at 0.1 MPa (broken line) and His81Mb derivative at 0.1 MPa (solid line). The residual of the single-exponential fitting is shown on the top of each decay signal. The experiments were performed at 293 K. The sample solution contained ca. 5 μM of ZnMb derivatives dissolved in 100 mM Tris−HCl, pH 7.4.

where ΔA_{380} is the absorbance change at 380 nm, A_1, A_2 and A_3 are constants, and t is the time (seconds). The first term, $A_1\{\exp(-k_{obs}t) - \exp(-k_b t)\}$, corresponds to the absorbance changes by the formation of Zn^+Mb. As well as Zn^+Mb, ^{3}Zn*Mb has significant absorbance at 380 nm (data not shown) and the second term, $A_2 \exp[-k_{obs}t]$, represents the contribution from the decay of ^{3}Zn*Mb. The triplet decay rate constant, k_{obs}, in eq 2 was fixed to the rate obtained from the absorbance decay at 450 nm.[23]

High-pressure laser flash photolysis measurements were performed using a steel pressure cell and its inner capsule made of quartz.[33] The optical square-shaped part has the path length of 4.0 or 5.0 nm. The pressure was transmitted from an intensifier (Hikari High-Pressure Co., Ltd. KP-5-B) and was measured by a Bourdon tube over a range from atmospheric pressure to 100 MPa. The sample temperature was controlled by using a circulating water bath arrangement. Each rate constant reported in this study is the average of 5−10 individual kinetic measurements at the stated pressure. High-pressure laser flash photolysis measurements were usually performed at pressure intervals of 20 MPa up to 100 MPa and down to 0.1 MPa again. After lowering the pressure to 0.1 MPa, the rate constants were confirmed to be the same as those before raising the pressure within the experimental error, which confirmed that the proteins were not denatured by pressurization. All experiments under high pressure were performed in 100 mM Tris−HCl, pH 7.4. pH of Tris buffer has been shown to be independent of pressure up to 200 MPa.[34]

Results

Kinetics at Ambient Pressure. To estimate the intrinsic decay rate for ^{3}Zn*Mb, k_d, the absorbance change at 450 nm was followed in the Ru-unmodified ZnMb sample after the pulsed-laser excitation (Figure 2: dotted curve). The rate constant (k_d), 50 s^{-1}, was obtained at 293 K in 100 mM Tris−HCl, pH 7.4, by fitting a single exponential function, which is virtually the same as that previously reported.[24] In one of the Ru−ZnMbs, His81Mb, the modification by the Ru complex accelerated the decay rate, as illustrated in Figure 2 (solid curve). Random residuals from a single-exponential fitting (solid line in the top of Figure 2) indicate that the decay of the triplet state in this Ru−ZnMb is monophasic. For other Ru−ZnMbs, His48Mb and His83Mb, the kinetic data can also be fit to a

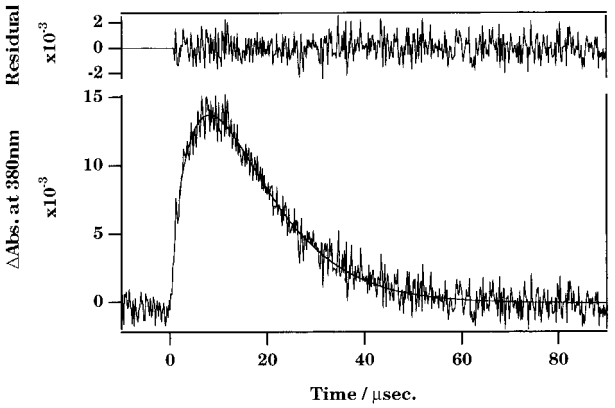

Figure 3. Charge recombination signal in the His48Mb derivative monitored at 380 nm. The sample solution contained ca. 5 μM of Ru−ZnMb derivatives dissolved in 100 mM Tris−HCl, pH 7.4 at 0.1 MPa. The residual of the fitting is shown on the top. The fitting procedure is described in the Materials and Methods.

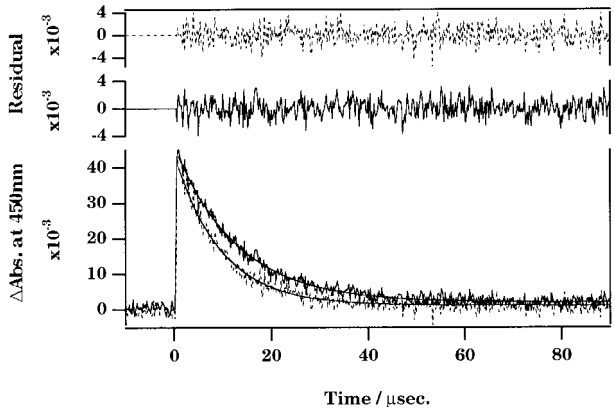

Figure 4. Transient absorbance changes at 450 nm obtained after laser excitation (532 nm; 10-ns pulse width) of His48Mb derivative at 0.1 MPa (broken line) and at 100 MPa (solid line). The residual of the single-exponential fitting is shown on the top of each decay signal. The experiments were performed at 293 K. The sample solution contained ca. 5 μM of ZnMb derivatives dissolved in 100 mM Tris−HCl, pH 7.4.

single-exponential expression. The rate constant (k_{obs}) was obtained as follows; 500 s^{-1}, 120 s^{-1}, and 9.90×10^4 s^{-1} for His83Mb, His81Mb, and His48Mb, respectively.

By subtracting the intrinsic decay rate constant, k_d, from the observed decay rate constants, k_{obs}, as shown in eq 1, the rate constant of the forward ET (k_f) at 293 K was calculated: 450 s^{-1}, 70 s^{-1}, and 9.90×10^4 s^{-1} for His83Mb, His81Mb, and His48Mb, respectively. The ET rate constants, k_f, were independent of sample concentration (2−5 μM) in all derivatives, showing that the observed ET reactions correspond to the intramolecular ET reactions, not to bimolecular ET reactions.[22,31]

These ET rate constants in this study are in good agreement with the results obtained by Gray and co-workers,[22,31] but not with the previous results reported in our laboratory.[11] In our previous study,[11] the laser experiments were performed after the samples were stirred for 30 min in a glovebox filled with argon gas, whereas we used vacuum argon line to completely remove dissolved oxygen from the samples for the present measurements. The Soret absorption band in the UV/vis spectrum did not exhibit any bleaching after the laser experiments (figure not shown). We also confirmed that the samples prepared by using the glovebox showed significant bleaching at the Soret band by the laser irradiation (result not shown), which indicates that the oxygen molecules cannot completely be removed from the sample solution by the previous experimental procedure. Since the dissolved O_2 molecule in the sample solution would quench the triplet state of ZnP,[19−21] the decay of ^{3}Zn*Mb was accelerated to give the larger "apparent" ET rate than the "real" ET rate from ^{3}Zn*Mb to protein-bound Ru^{3+} complex. We, therefore, concluded that the disagreement of the ET rates between our previous and current experiments can be ascribed to contamination of an oxygen molecule in the previous sample preparation and that current experimental procedure using argon-vacuum provides us with the "real" ET rates in Ru−ZnMbs.

After the intramolecular ET reaction from ^{3}Zn*Mb to $(NH_3)_5$-Ru^{3+}, the Ru^{2+}−Zn^+Mb intermediate is formed (Scheme 1). Since the free energy of Ru^{2+}−Zn^+Mb is higher than that of the initial state, Ru^{3+}−ZnMb (0.96 eV), the Ru^{2+}−Zn^+Mb intermediate returns to the initial state by the thermal electron−hole recombination reaction (back ET reaction) with a rate constant, k_b. Figure 3 shows the absorbance change at 380 nm for the His48Mb derivative. The decay signals at 380 nm were fitted by eq 2, and the residuals from the fitting curves were random. The rate constants, k_b, were obtained as follows: 580 s^{-1}, 40 s^{-1}, and 1.3×10^5 s^{-1} for His83Mb, His81Mb, and His48Mb, respectively. These rate constants, k_b, were also independent of the sample concentration, which confirms that the back ET reactions measured in this study are intramolecular ET reactions. The back ET rate constants for His48Mb and His83Mb have been reported by Casimiro et al.,[22] which is virtually the same as our results. The back ET rates for these two Ru−ZnMbs were larger than the corresponding forward ET rates, due to the higher redox potential for the back ET reactions (0.96 and 0.82 eV for the forward and back ET reactions, respectively). For His81Mb, however, the back ET rate was found to be slower (40 s^{-1}) than the forward ET rate (120 s^{-1}). Although reasons for the reversed ET rates to the redox potentials in this derivative are still unclear, this disconnection suggests that the redox potentials for His81Mb are deviated from those of other Ru−ZnMbs and/or that other factors regulating the ET reaction such as reorganization energy are significantly different between the forward and back ET reactions in His81Mb.

TABLE 1: Electron Transfer Rate Constants in Ru−ZnMbs at 0.1 and 100 MPa

	k_f, s^{-1}		k_b, s^{-1}	
	0.1 MPa	100 MPa	0.1 MPa	100 MPa
His83Mb	4.5×10^2	4.9×10^2	5.8×10^2	9.3×10^2
His81Mb	7.0×10^1	6.0×10^1	4.0×10^1	5.0×10^1
His48Mb	9.9×10^4	8.0×10^4	1.2×10^5	1.5×10^5

Kinetics at High Pressure. The ET rate constants in Ru−ZnMb (k_f, k_b) were measured up to 100 MPa at pressure intervals of 20 MPa. The typical absorbance decays for the forward ET process at 100 MPa for His48Mb are shown in Figure 4 (dotted curve). Even under high pressure, the residuals from a single-exponential fitting were random (dotted line in the top of Figure 4). To estimate the rate constants for the forward ET, k_f (eq 1), we also measured the rate constant, k_d, in Ru-unmodified ZnMb under high pressure. The rate constant, k_d, was slightly accelerated by pressurization; 50 s^{-1}, 52 s^{-1} at 0.1 and 100 MPa, respectively. The rate constants, k_f and k_b, at 0.1 and 100 MPa for Ru−ZnMb derivatives are summarized in Table 1.

In the forward ET reactions of the two Ru−ZnMbs, His81Mb and His48Mb, the rate constants, k_f, were decelerated by pressurization, while the slight acceleration was found for the reaction rate of another Ru−ZnMb, His83Mb. On the other hand, the rate constants for the back ET reactions (k_b) were

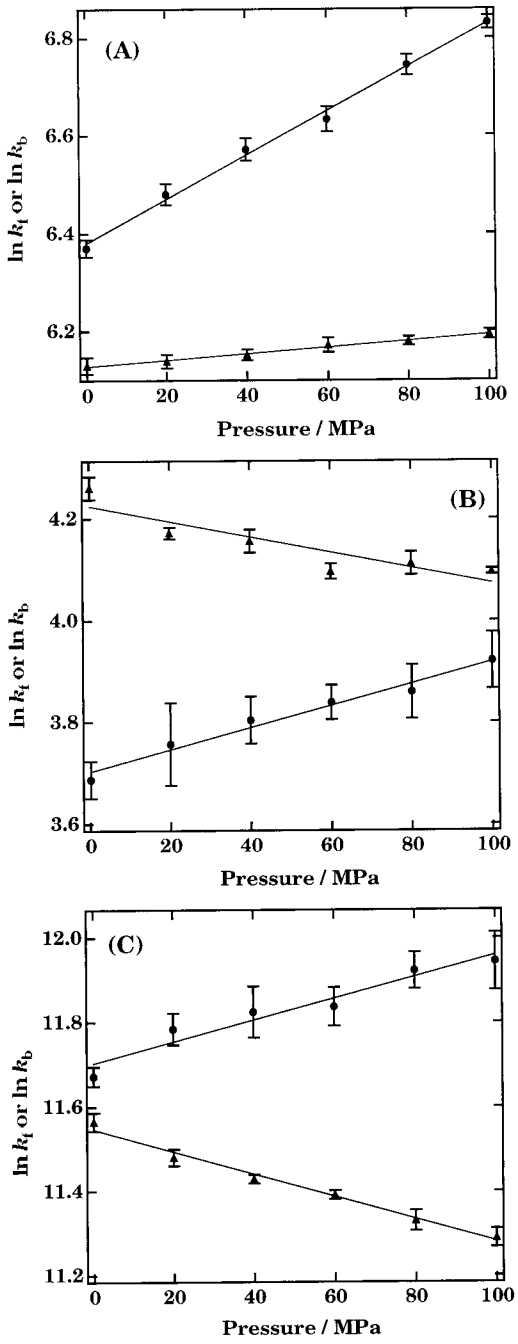

Figure 5. Pressure dependence of intramolecular ET rates in Ru−ZnMb derivatives: (A) His83Mb derivative; (B) His81Mb derivative; (C) His48Mb derivative. Solid lines are linear least-squares fits. Symbols: (▲) forward ET rate (^{3}ZnP* → Ru^{3+}) (●) back ET rate (Ru^{2+} → ZnP^+).

accelerated by pressurization in all derivatives. To quantitatively characterize the pressure dependence of the ET reactions in Ru−ZnMb derivatives, we estimated the activation volumes $\Delta V^{\neq}$ for the forward and back ET reactions, which are defined by the following equation.[14]

$$\left(\frac{\partial \ln k}{\partial P}\right)_T = -\frac{\Delta V^{\neq}}{RT} \quad (3)$$

where k is the rate constant, P is the pressure, R is the gas constant, and T is the temperature. As shown in Figure 5, the plot of the natural logarithm of the rate constants against the pressure was linear and the activation volumes were determined by the linear least-squares fitting. The activation volumes $\Delta V^{\neq}$ in each ET process are summarized in Table 2.

TABLE 2: Activation Volumes for the Forward and the Back ET Reactions

	$\Delta V^{\neq}_f$, cm^3/mol	$\Delta V^{\neq}_b$, cm^3/mol
His83Mb	-1.6 ± 0.2	-11 ± 0.5
His81Mb	$+3.7 \pm 0.1$	-5.3 ± 0.5
His48Mb	$+6.5 \pm 1.0$	-6.2 ± 0.5

As well as the ET rates at the ambient pressure, the pressure dependences of these Ru−ZnMbs are significantly different from those previously reported in our laboratory.[11] These differences can also be attributable to contamination of O_2 in the previous sample preparation. Since the kinetic measurements under elevated pressure have been done by raising pressure step by step from the ambient condition in our experimental procedure, the dissolved O_2 is consumed to form active oxygen species by accumulation of the laser irradiation in pressurization. The accelerating effect by the contaminated O_2 would, therefore, be less effective under high pressure, compared to that at the ambient pressure. Such deceleration in the decay of ^{3}Zn*Mb would slow the apparent ET rate by pressurization, which shifts the activation volume to the positive side (eq 3). In fact, the activation volumes previously reported were shifted to the positive side.[11] To avoid contamination of O_2, we used a vacuum-argon line in this study and confirmed no contribution of the quenching by dissolved O_2 to the decay of ^{3}Zn*Mb by showing that the apparent quantum yield of ^{3}Zn*Mb did not depend on number of the laser shots.

Discussion

Theoretical Basis for Analysis. According to the semiclassical ET theory,[1] the kinetics for long-range ET reactions have been shown to be mainly dependent on the following determinants: a D−A distance, d, a redox potential, $-\Delta G°$, a reorganization energy, λ, and electronic coupling at the closest contact (3 Å) between donor and acceptor, $H_{AB}°$. Rate constants for long-range protein ET reactions can be described by the following expression, the Marcus equation,[1]

$$k_{ET} = \frac{4\pi^2 (H_{AB}°)^2}{h(4\pi\lambda RT)^{1/2}} \exp[-\beta(d-3)] \exp\left[-\frac{(\Delta G° + \lambda)^2}{4\lambda RT}\right] \quad (4)$$

where β is the distance decay factor, which depends on the mediator between the redox centers. In the factors regulating ET rates, the previous studies[15−18,35] have shown that the reorganization energy, λ, the D−A distance, d, and free energy difference, $\Delta G°$, may be affected by pressurization.

One of these pressure-dependent parameters, the reorganization energy, λ, corresponds to the energy to reorganize the solvent or the reactant molecules during the redox reactions and mainly depends on the local environments around redox centers.[2] Although the estimation of the pressure-induced perturbation on the reorganization energy is not simple and difficult in protein ET reactions, the small contribution to pressure-induced alteration in the ET rates was reported in the organic molecules. Chung et al.[36] have estimated no pressure effects on the reorganization energy up to 256 MPa by the photoinduced bimolecular ET rates between some anthracene derivatives and simple alkyl-substituted benzene donors. In the present ET reactions, all of the Ru−ZnMb derivatives have the Ru-modified histidine residues on the protein surface and no significant environmental differences of the incorporated zinc porphyrins were found, implying that the reorganization energy would be

almost the same in these ET reactions. When the pressure dependence of these ET reactions is assumed to be governed by the pressure-induced perturbation on the reorganization energy, it is likely that three Ru−ZnMb derivatives exhibit the similar pressure dependence of the ET reactions due to their similar reorganization energies. As clearly shown in our results, however, the pressure dependence in these ET reactions was quite different. Recently, Miyashita and Go[37] reported the theoretical arguments on the pressure dependence of the ET reactions, also showing that contribution of pressure effects of λ on the ET reactions can be negligible. It would, therefore, be a good approximation that the contribution of λ to the pressure dependence of ET rates in Ru−ZnMb derivatives is small.

When the reorganization energy is almost insensitive to pressure or has quite small pressure dependence, the Marcus equation can be simplified to have only two pressure-dependent parameters, $\Delta G°$ and d. The pressure dependence of the ET rates, $(\partial \ln k/\partial P)_T$, can, therefore, be expressed as follows.

$$\left(\frac{\partial \ln k}{\partial P}\right)_T = -\beta\left(\frac{\partial d}{\partial P}\right)_T - \frac{2(\lambda + \Delta G°)}{4\lambda RT}\left(\frac{\partial \Delta G°}{\partial P}\right)_T \qquad (5)$$

Since $(\partial \ln k/\partial P)_T$ corresponds to $-\Delta V^{\neq}/RT$ (eq 3), eq 6 can be obtained. On the basis of the pressure dependence of the normal-mode analysis, Miyashita and Go also proposed[37] that the

$$\Delta V^{\neq} = \beta RT\left(\frac{\partial d}{\partial P}\right)_T + \left(\frac{\lambda + \Delta G°}{2\lambda}\right)\left(\frac{\partial \Delta G°}{\partial P}\right)_T \qquad (6)$$

activation volume can be expressed by the changes of the redox potential and the D−A distance, supporting the derivation of eq 6. In the following section, therefore, we will analyze the pressure dependence of the ET reaction rates based on eq 6 and discuss the pressure effects on the redox potential, $(\partial \Delta G°/\partial P)_T$, and D−A distance, $(\partial d/\partial P)_T$.

Pressure Effects on Redox Potential. Since the pressure effects on the redox potential, $(\partial \Delta G°/\partial P)_T$, correspond to the reaction volume, ΔV, and can be divided into two contributions from the redox centers, Ru complex and ZnP, the activation volumes for the forward and back ET reactions can be represented as follows:

$$\Delta V^{\neq}_{\mathrm{f}} = \beta RT\left(\frac{\partial d}{\partial P}\right)_T + \left(\frac{\Delta G°(k_{\mathrm{f}}) + \lambda}{2\lambda}\right)(\Delta V_{\mathrm{Ru^{3+}\rightarrow Ru^{2+}}} + \Delta V_{{}^3\mathrm{ZnP^*\rightarrow ZnP^+}}) \qquad (7)$$

and

$$\Delta V^{\neq}_{\mathrm{b}} = \beta RT\left(\frac{\partial d}{\partial P}\right)_T + \left(\frac{\Delta G°(k_{\mathrm{b}}) + \lambda}{2\lambda}\right)(\Delta V_{\mathrm{Ru^{2+}\rightarrow Ru^{3+}}} + \Delta V_{\mathrm{ZnP^+\rightarrow ZnP}}) \qquad (8)$$

In eq 7, the volume changes in the ZnP associated with the ET reactions, $\Delta V_{{}^3\mathrm{ZnP^*\rightarrow ZnP^+}}$, can separate into those of two processes, the photoexcitation, $\Delta V_{{}^3\mathrm{ZnP^*\rightarrow ZnP}}$ and the redox process, $\Delta V_{\mathrm{ZnP\rightarrow ZnP^+}}$. Thus, eq 7 can be further expressed as follows:

$$\Delta V^{\neq}_{\mathrm{f}} = \beta RT\left(\frac{\partial d}{\partial P}\right)_T + \left(\frac{\Delta G°(k_{\mathrm{f}}) + \lambda}{2\lambda}\right)(\Delta V_{\mathrm{Ru^{3+}\rightarrow Ru^{2+}}} + \Delta V_{{}^3\mathrm{ZnP^*\rightarrow ZnP}} + \Delta V_{\mathrm{ZnP\rightarrow ZnP^+}}) \qquad (9)$$

Equations 8 and 9 show that the activation volume for the ET reaction consists of the pressure dependence of the D−A distance and reaction volumes of the redox centers. To discuss the contributions of these factors to the activation volume, some assumptions have been employed to simplify these equations.

Among the five reaction volumes in eqs 8 and 9, the partial reaction volumes for the redox reactions on the Ru complex, $\Delta V_{\mathrm{Ru^{3+}\rightarrow Ru^{2+}}}$ and $\Delta V_{\mathrm{Ru^{2+}\rightarrow Ru^{3+}}}$ can be estimated by the redox reactions of Ru complexes under high pressure.[15,38] The volume changes by the reduction of $Ru(NH_3)_6^{3+}$ and $Ru(NH_3)_5$(isonicotinamide)$^{3+}$ are about 30 cm^3 mol^{-1}. On the other hand, the measurements for the reaction volumes associated with the photoexcitation, $\Delta V_{{}^3\mathrm{ZnP^*\rightarrow ZnP}}$, and the redox processes, $\Delta V_{\mathrm{ZnP^+\rightarrow ZnP}}$ and $\Delta V_{\mathrm{ZnP\rightarrow ZnP^+}}$, have not yet been examined, which complicates further analysis.

However, high-pressure voltammetry experiments for cytochrome *c* provide us with some estimations for the volume changes associated with the redox process of zinc porphyrin, $\Delta \bar{V}_{\mathrm{ZnP\rightarrow ZnP^+}}$ and $\Delta V_{\mathrm{ZnP^+\rightarrow ZnP}}$. The redox reaction for cytochrome *c*, in which ferric iron porphyrin is reduced to ferrous iron porphyrin, showed a rather small volume change (ca. 5 cm^3 mol^{-1}).[39] Although we used zinc as the metal center of porphyrin for Ru−ZnMbs and the reaction volume for the redox process of metal porphyrins might depend on the metal center, it is unlikely that the reaction volume for the redox process on ZnP in Ru−ZnMbs would drastically deviate from that on iron porphyrin in cytochrome *c*. The contribution of the activation volume for the redox process on ZnP is, therefore, much smaller than those of the Ru complex (ca. 30 cm^3 mol^{-1}). The small contribution of the volume change for the redox reaction on the heme group to the total apparent reaction volume is also supported by high-pressure pulse radiolysis experiments for Ru-modified cytochrome *c*.[16,17,38]

The volume changes for the photoexcitation process have been estimated for Zn-uroporphyrin, which are the only data available so far. By using a photoacoustic technique, Feitelson and Mauzerall[40] have reported that the volume of Zn-uroporphyrin is reduced for 1.5 cm^3 mol^{-1} by formation of the triplet state. This result suggests that the volume of the triplet excited state for ZnP in Ru−ZnMb is also smaller than that of the ground state and the contribution of the reaction volume for the photoexcitation to the activation volume, $\Delta V_{{}^3\mathrm{ZnP^*\rightarrow ZnP}}$, is less significant than the reaction volume for the redox changes in Ru complexes, $\Delta V_{\mathrm{Ru^{3+}\rightarrow Ru^{2+}}}$ (ca. 30 cm^3 mol^{-1}) in Ru−ZnMbs. In fact, $\Delta V_{{}^3\mathrm{ZnP^*\rightarrow ZnP}} + \Delta V_{\mathrm{ZnP\rightarrow ZnP^+}}$ in eq 9 would be about 3−4 cm^3 mol^{-1}, showing that the contributions of the volume changes in ZnP would be less than 15% of those in Ru complexes.

Under the condition that the volume changes for the ET reaction in Ru−ZnMbs can primarily be ascribed to that in the Ru complex, the activation volumes for the forward and back ET reactions, $\Delta V^{\neq}_{\mathrm{f}}$ and $\Delta V^{\neq}_{\mathrm{b}}$, can be expressed as follows:

$$\Delta V^{\neq}_{\mathrm{f}} = \beta RT\left(\frac{\partial d}{\partial P}\right)_T + \left(\frac{\Delta G°(k_{\mathrm{f}}) + \lambda}{2\lambda}\right)\Delta V_{\mathrm{Ru^{3+}\rightarrow Ru^{2+}}} \qquad (10)$$

$$\Delta V^{\neq}_{\mathrm{b}} = \beta RT\left(\frac{\partial d}{\partial P}\right)_T + \left(\frac{\Delta G°(k_{\mathrm{b}}) + \lambda}{2\lambda}\right)\Delta V_{\mathrm{Ru^{2+}\rightarrow Ru^{3+}}} \qquad (11)$$

To confirm the validity of the assumptions to simplify eqs 8 and 9 to eqs 10 and 11, we calculated the activation volume differences between the forward and back ET reactions by using eqs 10 and 11. In eqs 10 and 11, $\Delta V_{\mathrm{Ru^{3+}\rightarrow Ru^{2+}}} = -\Delta V_{\mathrm{Ru^{2+}\rightarrow Ru^{3+}}}$,

TABLE 3: D−A Distances, Changes of Redox Potentials and Distances Per 1 MPa, and Linear Compressibilities of Ru−ZnMb Derivatives

	d, Å	ΔV,[a] cm^3/mol	$(\partial\Delta G/\partial P)_T$, eV/MPa (x10^4)	$(\partial d/\partial P)_T$,[a] Å/MPa (x10^4)	κ, m^2/N (x10^{11})
His83Mb	15.5	25.8	2.67	-34 ± 1.0	22 ± 1.0
His81Mb	19.3	24.7	2.56	-9.9 ± 1.0	5.1 ± 0.5
His48Mb	12.7	34.8	3.61	$+3.3 \pm 4.1$	-2.6 ± 3.2

[a] Calculated by using $\Delta G^\circ(k_f) = -0.82$ eV, $\Delta G^\circ(k_b) = -0.96$ eV (ref 24), $\beta = 0.9$ Å^{-1} (ref 31), and $\lambda = 1.4$ eV (ref 2).

therefore,

$$\Delta V^{\neq}_f - \Delta V^{\neq}_b = \beta RT\frac{\partial}{\partial P}\{d(k_f) - d(k_b)\} + \left\{\frac{\Delta G^\circ(k_f) + \Delta G^\circ(k_b)}{2\lambda} + 1\right\}\Delta V \quad (12)$$

where $\Delta V = \Delta V_{Ru^{3+}\rightarrow Ru^{2+}}$. Since the D−A distance for the forward and back ET reactions, $d(k_f)$ and $d(k_b)$, are almost the same in the two ET processes,[2] eq 12 can be simplified to

$$\Delta V^{\neq}_f - \Delta V^{\neq}_b = \left\{\frac{\Delta G^\circ(k_f) + \Delta G^\circ(k_b)}{2\lambda} + 1\right\}\Delta V \quad (13)$$

By using eq 13, the volume changes, ΔV, for the ET reactions were found to be 34.8, 24.7, and 25.8 cm^3 mol^{-1}, for His48Mb, His81Mb, and His83Mb, respectively, as compiled in Table 3. Although these ΔV show some variations among three Ru−ZnMbs, they are close to those of the reduction of $Ru(NH_3)_6^{3+}$ (28.7 cm^3 mol^{-1})[15] and $Ru(NH_3)_5$(isonicotinamide)$^{3+}$ (33 cm^3 mol^{-1}).[38] Although the assumptions we employed for the derivation of eq 13 might be rough and oversimplified, correspondence between the estimated and observed reaction volume for the redox process on the Ru complex indicates that the assumptions we employed for the derivation of eq 13 would be valid, and it can safely be concluded that, in the ET reactions of Ru−ZnMb examined here, the pressure dependence of the redox potential, $(\partial\Delta G^\circ/\partial P)_T$, can mainly be attributable to the pressure-induced changes in the redox potential of the Ru complex.

Pressure Dependence of Donor−Acceptor Distance. To estimate the pressure dependence of the D−A distance, we utilized eq 6 with the parameters shown in Table 3, and the resultant $(\partial d/\partial P)_T$ are summarized. As clearly shown in Table 3, it should be noted here that the pressure dependence of the D−A distance, $(\partial d/\partial P)_T$, is dependent on the position of the Ru-complex, which is in sharp contrast to the pressure dependence of the redox potential, $(\partial\Delta G^\circ/\partial P)_T$. Both of His81Mb and His83Mb exhibited negative $(\partial d/\partial P)_T$, corresponding to the compression of the donor−acceptor distance by pressure. The negative $(\partial d/\partial P)_T$ for these two Ru−ZnMbs are comparable to the average distance change in BPTI[41] (-2.5×10^{-4} Å MPa^{-1}). Although high-resolution two-dimensional NMR spectroscopy for Mb has not yet been reported under high pressure, the comparable $(\partial d/\partial P)_T$ for these myoglobin systems to that for BPTI imply that the estimation of the pressure-induced structural changes by the high-pressure flash photolysis for the ET reaction would be reasonable.

In the other Ru−ZnMb, His48Mb, however, $(\partial d/\partial P)_T$ was a small positive value with rather large experimental error,[42] indicating that the pressure-induced distance change in this ET reaction is small or nearly zero. The site-dependent pressure induced compression was also suggested by the high pressure study on BPTI. Li et al.[41] reported that a hydrogen bond between the amide proton and the carbonyl oxygen changes its distance by pressure in the range between -5.5×10^{-4} and $+0.5 \times 10^{-4}$ Å MPa^{-1}. The pressure effects on the D−A distance are, therefore, not unique but depend on the position of the redox center.

To gain further insight into the pressure dependence of the D−A distance and discuss the heterogeneity of the $(\partial d/\partial P)_T$ for three myoglobin systems, the pathway analysis[43,44] for the ET reactions is crucial. Some ET pathways in Ru−ZnMbs have already been examined by Cowan et al.,[45] and those in His81Mb and His48Mb are shown in Figure 6. In the His48Mb derivative, an electron is transferred through the covalent bond between His 48 and Arg 45 and, then, moves to the ZnP via the hydrogen bond between Arg 45 and propionate of ZnP. While the His48Mb derivative has only one hydrogen bond in its ET pathway, the ET reaction in His81Mb is mediated by many hydrogen bonds. As illustrated in Figure 6, His 81 is located near the end of the F-helix and an electron would be transferred along the F-helix to Ser 92 at the other end of the helix.

The most prominent difference between the two ET pathways is the number of hydrogen bonds, which would differentiate the pressure dependence of the ET reactions. Previous studies[41] have revealed that hydrogen bonds are easily shortened by pressurization, which accelerates the ET reaction. In the present high-pressure experiments, the ET reaction rate in His81Mb was significantly increased by pressurization. On the other hand, the ET reaction through the covalent bonds has shown to be pressure-resistant[18] and the pressure dependence of the ET reaction in Ru-modified cytochrome b_5, which has a typical ET reaction mediated by covalent bonds, was quite small and the activation volume was nearly zero. The ET pathway in His48Mb is mainly constructed by the covalent bonds and only one hydrogen bond is included, which results in the pressure-resistant ET reaction rate. Although the ET pathway in His83Mb has not been examined, it is likely that an electron would also be transferred through the F-helix by many hydrogen bonds as found for His81Mb, leading to the large and negative pressure dependence of the D−A distance.

However, the pressure dependence of the D−A distance in His83Mb was more pronounced than that in His81Mb. It is quite interesting and informative that the pressure dependence of the ET reaction is sensitive to the slight structural deviation of the position of the redox center. As shown in Figure 6, the ET pathways in His81Mb and His83Mb appear to be quite similar, constructed by many hydrogen bonds. His 81 is one of the intrinsic histidine residues on the protein surface forming a hydrogen bond between N_δ of His 81 and carbonyl group of the backbone (Lys 78), which would fix the orientation of the imidazole ring of His 81. Although His 83 is located near His 81 and would also be exposed to the solvent, the position of 83 is originally occupied by glutamic acid in native protein and no hydrogen bonds would be formed to fix the imidazole ring of His 83. It is more plausible that the hydrogen bond observed for the side chain of His 81 restricts the thermal fluctuation around His 81, resulting in the reduced pressure perturbation on the D−A distance for His81Mb. The local structural fluctuation would, therefore, affect the dynamic properties of the ET reaction.

Protein Fluctuation. In the previous study,[11] we reported that the activation volumes of the ET reactions in all of the Ru−ZnMb derivatives were positive, which was monotonically increased as the donor and acceptor sites were more separated. On the basis of these observations, in the previous study, we

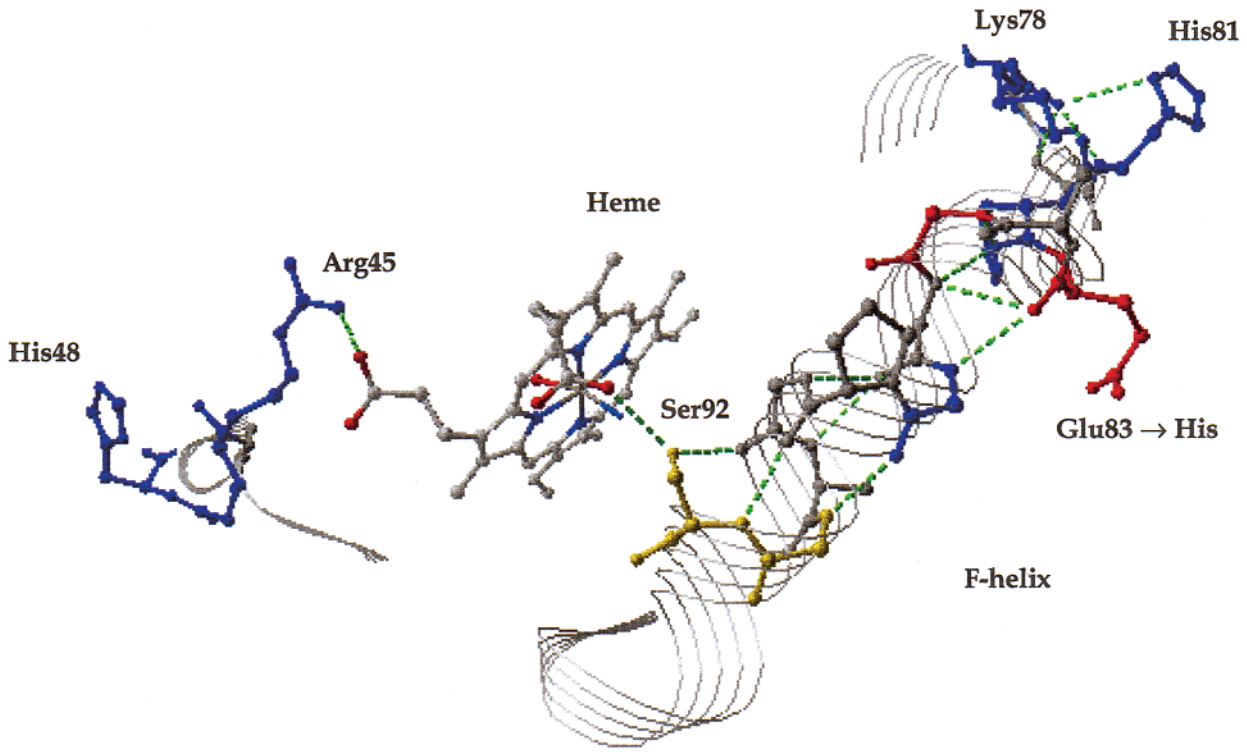

Figure 6. Partial structure of human myoglobin showing heme ring and residues 78−92 and 45−48. Dotted lines show the hydrogen bonds.

introduced the effect of protein thermal fluctuation into the electronic coupling term, H_{AB} ($=(H_{AB}^{o})^2 \exp[-\beta(d-3)]$), of the Marcus equation (eq 4). Due to the structural fluctuation, the actual ET distance (r) in proteins would fluctuate around the D−A distance (d) estimated from the X-ray crystal structure. Supposing that the potential energy surface in the protein structural fluctuation is $\alpha(r-d)^2$, where α is the curvature coefficient in the coordinate of the protein structural fluctuation, the electronic coupling term, H_{AB}, should be averaged over the Boltzmann factor, $\exp[-\alpha(r-d)^2/kT]$. The resulting Marcus equation is given by

$$k = \frac{4\pi^2(H_{AB}^{\circ})^2}{h(4\pi\lambda RT)^{1/2}} \exp\left[-\beta d + \frac{kT\beta^2}{4\alpha}\right] \exp\left[-\frac{(\lambda+\Delta G^{\circ})^2}{4\lambda RT}\right] \quad (14)$$

In this equation, the factor $\exp(kT\beta^2/4\alpha)$ comes from the contribution of the thermal average and is referred to as the thermal fluctuation factor. Under high pressure,[12−14] the hydrostatic compression increases material density and suppresses the thermal fluctuation and fluctuation width, corresponding to the increase of the curvature coefficient, α, in the potential energy surface of the protein structural fluctuation. The increased α by pressurization would depress the ET rate (eq 14) and lead to the positive activation volume (eq 3), even when the pressure effects on ΔG° and λ are negligible. This equation also explains the D−A distance dependence of the activation volume in the previous paper, since α is more substantially affected by pressurization at the larger D−A distances that leads to the larger changes in the rate constant.

As mentioned in the Introduction and Results, however, the previous activation volumes contained the contributions from the dissolved O_2. The present experiments under complete anaerobic conditions show that a negative activation volume for the forward ET reaction ($\Delta V^{\neq}_{f}$) was observed for His83Mb, and His81Mb, of which D−A distance is longer than that of His48Mb, exhibited a smaller $\Delta V^{\neq}_{f}$ than His48Mb. These refined experimental results in the present study clearly indicate that our previous proposal for effects of the thermal fluctuation on ET reactions should be reexamined. As discussed in the previous section, the positive activation volumes can be attributable to the pressure dependence of the redox potential without introduction of the "thermal fluctuation factor" into the Marcus equation. It is, therefore, still premature to conclude that the introduction of the Boltzmann factor to the Marcus equation can describe the dynamic properties of the ET reaction in proteins, particularly the contribution of the thermal fluctuation to the ET reaction (eq 14), but the present high pressure study has revealed that the effects of the thermal fluctuation on the ET reactions are dependent on the ET pathway and microenvironments of the redox center.

For the quantitative interpretation of the protein fluctuation, we utilize linear compressibility, κ (eq 15), which has been one of the useful indicators for protein fluctuation,[46−48] where d_0 is

$$\kappa = -\frac{1}{d_0}\left(\frac{\partial d}{\partial P}\right)_T \quad (15)$$

the donor−acceptor distance at 0.1 MPa. On the basis of values of $(\partial d/\partial P)_T$, κ was calculated as follows: $(2.1 \pm 0.1) \times 10^{-10}$, $(5.1 \pm 1.0) \times 10^{-11}$, and $(-2.6 \pm 3.2) \times 10^{-11}$ m^2 N^{-1} for His83Mb, His81Mb, and His48Mb, respectively (Table 3). By the normal-mode analysis, the average value of κ for all pairs of C^{α} atoms in sperm whale deoxy Mb was calculated to be 4.21×10^{-11} m^2 N^{-1}, which is comparable to our estimation.

As listed in Table 3, the linear compressibility also exhibits a clear dependence on the ET pathway. Both His81Mb and His83Mb, of which ET reactions are mediated by many hydrogen bonds, have positive linear compressibility, while negative and small linear compressibility was found for His48Mb, in which the ET pathway was mainly constructed by covalent bonds. As previously suggested,[15,18,49,50] bond angles and distances of hydrogen bonds are much more susceptible to the motion of the protein, compared to those of covalent bonds.

It would be quite reasonable to conclude that the structural fluctuation preferentially affects the ET process via hydrogen bonds, not via covalent bonds.

Even in His81Mb and His83Mb, significant deviation was evident in their linear compressibility. As discussed in the previous section, the mobility of the side chain of His 81 is reduced by formation of a hydrogen bond with backbone, which restricts the local structural fluctuation of the Ru complexes and reduces the linear compressibility. These heterogeneities in the structural fluctuation based on the slight difference of the microenvironments were also suggested by the theoretical simulation under high pressure.[51]

While relationships between the protein fluctuation and the ET reaction are still open to be solved, the present results from the ET reaction under high pressure strongly suggest that the structural fluctuation preferentially affects the ET process mediated by hydrogen bonds and is one of the key factors in the mechanism of protein ET reactions. Also, we proposed that the structural fluctuation is not unique in the protein structure and subtle difference in the microenvironments around the ET pathway would lead to significant alteration in the dynamic aspects of the ET reaction. To gain further insight into the fluctuation controlled ET mechanism, extensive studies on temperature and viscosity dependence of the ET reaction are now undergoing.

Acknowledgment. This work was supported by a grant from Ministry of Education, Science, Culture, and Sports (to I.M. and K.I., No. 11480191). We are grateful to Prof. S. G. Boxer and Dr. R. Varadarajan (Stanford University) for a gift of the expression vector of the human myoglobin gene. We are also greatly indebted to Messers Yoichi Sugiyama and Manabu Teramoto for some protein preparations, Dr. Shinichi Adachi at RIKEN for some mutant gene constructions, and Dr. Satoshi Takahashi for laser experiments. We are also obligated to Mr. Osamu Miyashita at Kyoto University for theoretical discussions.

References and Notes

(1) Marcus, R. A.; Sutin, N. *Biochim. Biophys. Acta* **1985**, *811*, 265−322.
(2) Winkler, J. R.; Gray, H. B. *Chem. Rev.* **1992**, *92*, 369−379.
(3) McLendon, G.; Hake, R. *Chem. Rev.* **1992**, *92*, 481−490.
(4) Hoffman, B. M.; Ratner, M. A. *J. Am. Chem. Soc.* **1987**, *109*, 6237−6243.
(5) McMahon, B. H.; Müller, J. D.; Wraight, C. A.; Nienhaus, G. U. *Biophys. J.* **1998**, *74*, 2567−2587.
(6) Medvedev, E. S.; Stuchebrukhov, A. A. *J. Chem. Phys.* **1997**, *107*, 3821−3831.
(7) Aquino, A. J. A.; Beroza, P.; Reagan, J.; Onuchic, J. N. *Chem. Phys. Lett.* **1997**, *275*, 181−187.
(8) Daizadeh, I.; Medvedev, E. S.; Stuchebrukhov, A. A. *Proc. Natl. Acad. Sci. U.S.A.* **1997**, *94*, 3703−3708.
(9) Frauenfelder, H.; Parak, F.; Young, R. D. *Annu. Rev. Biophys. Biochem.* **1988**, *17*, 451.
(10) Ansari, A.; Berendzen, J.; Bowne, S. F.; Frauenfelder, H.; Iben, I. E. T.; Sauke, T. B.; Shyamsunder, E.; Young, R. D. *Proc. Natl. Acad. Sci. U.S.A.* **1985**, *82*, 5000−5004.
(11) Sugiyama, Y.; Takahashi, S.; Ishimori, K.; Morishima, I. *J. Am. Chem. Soc.* **1997**, *119*, 9582−9583.
(12) Heremans, K.; Smeller, L. *Biochim. Biophys. Acta* **1998**, *1386*, 353−370.
(13) Frauenfelder, H.; Alberding, N. A.; Ansari, A.; Braunstein, D.; Cowen, B. R.; Hong, M. K.; Iben, I. E. T.; Johnson, J. B.; Luck, S.; Marden, M. C.; Mourant, J. R.; Ormos, P.; Reinisch, L.; Scholl, R.; Schulte, A.; Shyamsunder, E.; Sorensen, L. B.; Steinbach, P. J.; Xie, A.; Young, R. D.; Yue, K. T. *J. Phys. Chem.* **1990**, *94*, 1024−1037.
(14) Drljaca, A.; Hubbard, C. D.; van Eldik, R.; Asano, T.; Basilevsky, M. V.; le Noble, W. J. *Chem. Rev.* **1998**, *98*, 2167−2289.
(15) Meier, M.; van Eldik, R.; Chang, I.-J.; Mines, G. A.; Wuttke, D. S.; Gray, H. B. *J. Am. Chem. Soc.* **1994**, *116*, 1577−1578.
(16) Wishart, J. F.; van Eldik, R.; Sun, J.; Su, C.; Isied, S. S. *Inorg. Chem.* **1992**, *31*, 3986−3989.
(17) Sun, J.; Su, C.; Meier, M.; Isied, S. S.; Wishart, J. F.; van Eldik, R. *Inorg. Chem.* **1998**, *37*, 6129−6135.
(18) Scott, J. R.; Fairris, J. L.; McLean, M.; Wang, K.; Sligar, S. G.; Durham, B.; Millett, F. *Inorg. Chim. Acta* **1996**, *243*, 193−200.
(19) Barboy, N.; Feitelson, J. *Biochemistry* **1987**, *26*, 3240−3244.
(20) Feitelson, J.; McLendon, G. *Biochemistry* **1991**, *30*, 5051−5055.
(21) Papp, S.; Vanderkooi, J. M.; Owen, C. S.; Holtom, G. R.; Phillips, C. M. *Biophys. J.* **1990**, *58*, 177−186.
(22) Casimiro, D. R.; Wong, L.; Colon, J. L.; Zewert, T. E.; Richards, J. H.; Chang, I.-J.; Winkler, J. R.; Gray, H. B. *J. Am. Chem. Soc.* **1993**, *115*, 1485−1489.
(23) Elias, H.; Chou, M. H.; Winkler, J. R. *J. Am. Chem. Soc.* **1988**, *110*, 429−434.
(24) Cowan, J. A.; Gray, H. B. *Inorg. Chem.* **1989**, *28*, 2074−2078.
(25) Ford, P.; Rudd, D. F. P.; Gaunder, R.; Taube, H. *J. Am. Chem. Soc.* **1968**, *90*, 1187−1194.
(26) Adler, A. D.; Longo, F. R.; Kampas, F.; Kim, J. *J. Inorg. Nucl. Chem.* **1970**, *32*, 2443−2445.
(27) Varadarajan, R.; Szabo, A.; Boxer, S. G. *Proc. Natl. Acad. Sci. U.S.A.* **1985**, *82*, 5681−5684.
(28) Varadarajan, R.; Lambright, D. G.; Boxer, S. G. *Biochemistry* **1989**, *28*, 3771−3781.
(29) Adachi, S.; Sunohara, N.; Ishimori, K.; Morishima, I. *J. Biol. Chem.* **1992**, *267*, 12614−12621.
(30) Teale, F. W. J. *Biochim. Biophys. Acta* **1959**, *35*, 543.
(31) Axup, A. W.; Albin, M.; Mayo, S. L.; Crutchley, R. J.; Gray, H. B. *J. Am. Chem. Soc.* **1988**, *110*, 435−439.
(32) Everest, A. M.; Wallin, S. A.; Stemp, E. D. A.; Nocek, J. M.; Mauk, A. G.; Hoffman, B. M. *J. Am. Chem. Soc.* **1991**, *113*, 4337−4338.
(33) Hara, K.; Morishima, I. *Rev. Sci. Instrum.* **1988**, *59*, 2397−2398.
(34) Newmann, R. C. Jr.; Kauzmann, W.; Zipp, A. *J. Phys. Chem.* **1973**, *77*, 2687−2691.
(35) Freiberg, A.; Ellervee, A.; Tars, M.; Timpmann, K.; Laisaar, A. *Biophys. Chem.* **1997**, *68*, 189−205.
(36) Chung, W.; Turro, N. J.; Gould, I. R.; Farid, S. *J. Phys. Chem.* **1991**, *95*, 7752−7757.
(37) Miyashita, O.; Go, N. *J. Phys. Chem. B* **1999**, *103*, 562−571.
(38) Bänsch, B.; Meier, M.; Martinez, P.; van Eldik, R.; Su, C.; Sun, J.; Isied, S. S.; Wishart, J. F. *Inorg. Chem.* **1994**, *33*, 4744−4749.
(39) Sun, J.; Wishart, J. F.; van Eldik, R.; Shalders, R. D.; Swaddle, T. W. *J. Am. Chem. Soc.* **1995**, *117*, 2600−2605.
(40) Feitelson, J.; Mauzerall, D. *J. Phys. Chem.* **1996**, *100*, 7698−7703.
(41) Li, H.; Yamada, H.; Akasaka, K. *Biochemistry* **1998**, *37*, 1167−1173.
(42) Since the absorbance at 450 or 380 nm in His48Mb decays about 1000 times faster than those in the other derivatives, the noise was relatively enhanced for the measurements in His48Mb.
(43) Skourtis, S. S.; Regan, J. J.; Onuchic, J. N. *J. Phys. Chem.* **1994**, *98*, 8, 3379−3388.
(44) Beratan, D. N.; Onuchic, J. N.; Hopfield, J. J. *J. Chem. Phys.* **1987**, *86*, 4488−4498.
(45) Cowan, J. A.; Upmacis, R. K.; Beratan, D. N.; Onuchic, J. N.; Gray, H. B. *Ann. N. Y. Acad. Sci.* **1989**, *550*, 68−84.
(46) Cooper, A. *Proc. Natl. Acad. Sci. U.S.A.* **1976**, *73*, 2740−2741.
(47) Gekko, K.; Hasegawa, Y. *Biochemistry* **1986**, *25*, 6563−6571.
(48) Gekko, K.; Hasegawa, Y. *J. Phys. Chem.* **1989**, *93*, 426−429.
(49) Pudlak, M. *J. Chem. Phys.* **1998**, *108*, 5621−5625.
(50) Sumi, H.; Marcus, R. A. *J. Chem. Phys.* **1986**, *84*, 4894−4914.
(51) Yamato, T.; Higo, J.; Seno, Y.; Go, N. *Proteins: Struct., Function, Genet.* **1993**, *16*, 327−340.